Princeton Plasma Physics Laboratory

PPPL- 4520

PPPL- 4520

Optimizing Stellerators for Turbulent Transport

H.E. Mynick, N.Pomphrey, and P. Xanthopoulos

January 2008

Prepared for the U.S. Department of Energy under Contract DE-AC02-76CH03073.

Optimizing stellarators for turbulent transport

H.E. Mynick[1], N.Pomphrey[1], and P. Xanthopoulos[2]
[1]*Plasma Physics Laboratory, Princeton University, Princeton, NJ*
[2]*Max-Planck-Institut für Plasmaphysik, Teilinstitut Greifswald, Greifswald, Germany*

Up to now, the term "transport-optimized" stellarators has meant optimized to minimize neoclassical transport, while the task of also mitigating turbulent transport, usually the dominant transport channel in such designs, has not been addressed, due to the complexity of plasma turbulence in stellarators. Here, we demonstrate that stellarators can also be designed to mitigate their turbulent transport, by making use of two powerful numerical tools not available until recently, namely gyrokinetic codes valid for 3D nonlinear simulations, and stellarator optimization codes. A first proof-of-principle configuration is obtained, reducing the level of ion temperature gradient turbulent transport from the NCSX baseline design by a factor of about 2.5.
PACS #s: 52.55.Hc, 52.65.Tt, 52.35.Ra

Transport due to plasma turbulence has been a major challenge for magnetic confinement since the inception of the fusion program in the 1950s. Starting in the 1980s, a number of of approaches to neoclassical-transport-optimized stellarators were discovered[1–5], in which the neoclassical (nc) transport could be reduced to below the level of turbulent or "anomalous" transport over most of the plasma column, making stellarator confinement comparable to that achievable in tokamaks. In recent years, two powerful numerical tools have been developed, which also make mitigating turbulent transport in stellarators a realistic possibility, namely configuration optimization codes such as Stellopt[6], and gyrokinetic (gk) codes valid for 3D configuations, such as the GENE/GIST code package[7, 8]. In this paper, we make use of these two new tools to demonstrate that new stellarator configurations with appreciably diminished turbulent transport levels can be evolved from stellarators designed without this turbulent-transport-optimization, raising the prospect of a new class of stellarators with greatly improved overall confinement.

Stellopt seeks to minimize a cost function $C^2(\mathbf{z}) = \sum_i w_i^2 C_i^2(\mathbf{z})$ in the "shape space" $\mathbf{z} \equiv \{z_j\}$ specifying a stellarator design, where the C_i^2 are the contributions from any physics or engineering criteria the user wishes to apply, and the w_i are adjustable weights. (For the fixed-boundary equilibria we compute here, the z_j are the Fourier amplitudes specifying the boundary shape of the design. One could equally well take free-boundary equilibria, with the z_j the currents in the coil set.) For the turbulent contribution C_t^2, one could ideally take $C_t = \langle Q_{gk} \rangle$, the surface- or volume- averaged heat flux Q_{gk} from nonlinear GENE runs, but this would be far too computationally expensive, since many hundreds of individual configurations are evaluated in a typical optimizer run, and a nonlinear gk parallel simulation for a single flux tube for the present application requires on the order of 100 CPU-days. To surmount this obstacle, we instead employ a "proxy function" Q_{prox} in C_t^2 to stand in place of Q_{gk}, a fairly simple function of key input geometric quantities, based on theory and on the geometry dependences of Q_{gk} found in GENE studies on a family of nc-optimized stellarators.[9] Q_{prox} need not give a highly accurate prediction of what the gk result will be (though of course the more accurate the better) – it need only capture enough of the physics to guide the optimizer toward configurations which GENE will subsequently confirm has reduced Q_{gk}. Moreover, by examining the means by which Stellopt contrives to improve Q_{prox} and Q_{gk}, one may learn methods for deforming the stellarator shape to achieve the turbulent stabilization which are geometrically possible, whose discovery without the optimizer would be extremely difficult.

For Q_{prox}, we begin with an expression for the ion radial heat flux $Q_i = -\chi n_0 g^{xx} dT_i/dx$, with radial coordinate $x \equiv (2\psi_t/B_a)^{1/2}$, $2\pi\psi_t$ the toroidal flux, B_a the magnetic field strength B at the plasma edge (where $x = a$), and $g^{xx} \equiv |\nabla x|^2$ the xx component of the metric tensor. We use the quasilinear expression for the ion conductivity, $\chi = \sum_{\mathbf{k}} D_{\mathbf{k}}$, with

$$D_{\mathbf{k}} = (\omega_{*i} L_n)^2 \langle |\frac{e\phi_{\mathbf{k}}}{T_i}|^2 \rangle \gamma_{\mathbf{k}}/\omega_{\mathbf{k}}^2 \simeq c_D \gamma_{\mathbf{k}}/k_x^2. \qquad (1)$$

Here, $\omega_{*i} \equiv -(ck_y T_i/eB)\kappa_n$ is the diamagnetic frequency, with inverse density scale-length $\kappa_n \equiv L_n^{-1} \equiv -\partial_x \ln n_0$ and $k_y \equiv \mathbf{k}\cdot\hat{y}$ the wavevector component in the binormal direction $\hat{y} \equiv \hat{b} \times \hat{x}$, with $\hat{x}$ and $\hat{b}$ unit vectors in the directions normal to a flux surface and along the magnetic field. The final form is obtained using a simple mixing-length argument for the mean-square potential fluctuation amplitude $\langle |\phi_{\mathbf{k}}|^2 \rangle$, with c_D a multiplicative constant, determined below.

As in Ref. 9, for simplicity we consider only ion temperature gradient (ITG) turbulence[10] with adiabatic electrons. As found there, two geometric quantities central to determining the form and amplitude of the turbulence are the "radial curvature" $\kappa_1 \equiv \mathbf{e}_x \cdot \boldsymbol{\kappa}$, with vector curvature $\boldsymbol{\kappa}$ and $\mathbf{e}_x$ the covariant basis vector for x,[8] and the local shear $s_l \equiv \partial_\theta (g^{xy}/g^{xx})$, with θ the poloidal azimuth in flux coordinates, which parametrizes distance along a field line. An approximate ITG dispersion equation is

$$0 \simeq \frac{1}{\tau} + \frac{\omega_{*i}(1+\eta_i)\omega_{di}}{\omega^2} + \frac{k_\parallel^2 v_i^2 \omega_{*i}(1+\eta_i)}{\omega^3}, \qquad (2)$$

with $\omega_{di} = -\omega_{*i}\kappa_1/\kappa_n$ the ion drift frequency, $\eta_i \equiv \kappa_T/\kappa_n$, and $\kappa_T \equiv -\partial_x \ln T_i$. The first term on the right side is the adiabatic electron contribution, the second term gives the ITG "toroidal branch", and the third term gives the "slab branch". If that 3rd term is neglected, Eq.(2) is quadratic in ω, giving $\omega \equiv \pm i\gamma_{\mathbf{k}} \simeq \pm\omega_{*i}[\tau(1+\eta_i)\kappa_1/\kappa_n]^{1/2}$, becoming unstable for $\kappa_1 < 0$ ("bad curvature"). This expression has a critical pressure gradient $\kappa_{cr} = 0$, which becomes nonzero for a more complete dispersion equation, *e.g.*, from including the 3rd term in Eq.(2). Here, we include κ_{cr} simply as a parameter, by making the replacement $(1+\eta_i) \equiv \kappa_p/\kappa_n \rightarrow (\kappa_p - \kappa_{cr})/\kappa_n$. Then one has

$$\gamma_{\mathbf{k}} \simeq (\omega_{*i}/\kappa_n)|\tau\kappa_1(\kappa_p - \kappa_{cr})|^{1/2} H(\kappa_p - \kappa_{cr}) H(-\kappa_1), \quad (3)$$

with $H(\kappa)$ the Heavyside function. Retaining the 3rd term in Eq.(2), and making the replacement $k_\parallel \rightarrow -(i/qR)\partial_\theta$ (with R the major radius and q the safety factor) yields a Schrödinger equation, which localizes the mode in θ to wells in the effective potential $V_{ef}(\theta)$, proportional to the first two terms in Eq.(2).[9]

We model k_x^{-2} on the intuition that s_l plays a role similar to that played by flow shear,[9] stabilizing the mode and diminishing its radial extent from the "mesoscale" ($k_x^{-1} \sim \sqrt{L_p\rho_i}$) to a microscale ($k_x^{-1} \sim \rho_i$) when the $E \times B$ shearing frequency ω_E becomes comparable to the inverse correlation time τ_E^{-1} for fluctuations in the absence of $E \times B$ flow[11]:

$$k_x^{-2}(\omega_E, s_l) \simeq \rho_i^2 + \rho_i L_p/[1 + (\tau_E\omega_E)^2 + \langle(\tau_s s_l)^2\rangle_{\Delta\theta}]. \quad (4)$$

Here, ρ_i is the ion gyroradius, $L_p \equiv \kappa_p^{-1}$, τ_E, τ_s are constants set below, and $\langle..\rangle_{\Delta\theta}$ is an average along a field line weighted by a gaussian of width $\Delta\theta$, a simple means of giving k_x^{-2} the nonlocal character more rigorously imposed by actually solving the mode equation noted above along $\mathbf{B}$. Q_{prox} is thus determined by Eqs.(1),(3), and (4), which have 5 as yet undetermined constants, $\kappa_{cr}, \tau_E, \tau_s, \Delta\theta$, and c_D. Here, we neglect the flow-shear contribution (we set $\tau_E = 0$), and fix the remaining 4 by using simulated annealing[12] to make a best fit of Q_{prox} with the Q_{gk} from the results of GENE simulations on the family of 3 flux tubes in each of 4 toroidal configurations studied in Ref. 9, giving values 0.053, 1.12, 0.207, and 0.959, respectively. A comparison of Q_{prox} (solid) and Q_{gk} (dashed) along one field line of each of these 4 configurations is given in Fig. 1. For all flux tubes simulated, Q_{prox} represents reasonably well the form of Q_{gk} along $\mathbf{B}$, and also gives the approximate magnitude in each case but for 2 of the 3 tubes simulated for W7X (Wendelstein VII-X)[13], where it is too small by a factor of about 3, indicating that some further physics is to be found to improve the present Q_{prox}. The predictive reliability of C_t^2 is somewhat better than that indicated in Fig. 1, since it uses the surface average $\langle Q_{prox}\rangle$ of Q_{prox}, and the local disparities in $(Q_{prox} - Q_{gk})$ tend to cancel.

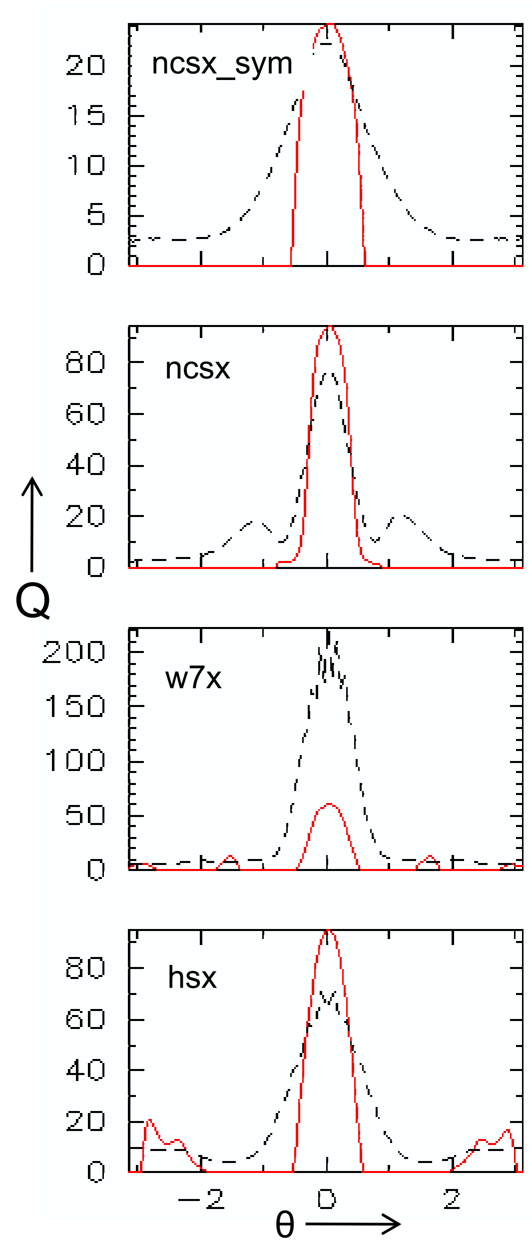

FIG. 1: (Color online)Comparison of Q_{prox} (red solid) with Q_{gk} (black dashed) for one flux tube of each of the 4 toroidal configurations studied in Ref. 9.

The results of a Stellopt run using this Q_{prox} are shown in Fig. 2 – Fig. 4. The Levenberg-Marquardt optimization scheme[14] Stellopt uses runs in successive "generations" of equilibria, here each with 54 members (one for each direction of shape space $\mathbf{z}$), to determine the direction in $\mathbf{z}$-space to move next. For this case, Stellopt begins with configuration LI383, which formed the baseline configuration for NCSX (National Compact Stellarator Experiment)[15], at $\beta = 4.2\%$. w_t is made large enough to make C_t^2 dominate C^2 for the first several generations. Constraints are also applied to maintain the plasma β,

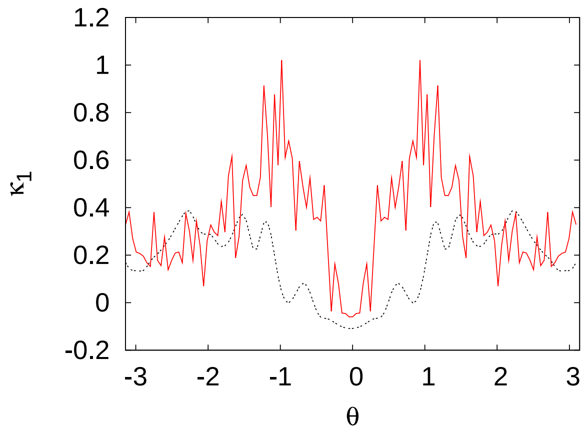

FIG. 2: (Color online) Comparison of radial curvature $\kappa_1(\theta)$ for 1 poloidal transit for QA_35q (red solid) and NCSX (black dashed).

aspect ratio, and RB_t (= major radius × toroidal field), but the configurations are otherwise unconstrained. After the 4^{th} generation, a sample equilibrium is chosen, before the configurations become less interesting from a practical standpoint (for example, their rotational transform dropping excessively). Here, we select a sample configuration "QA_35q" from that generation, whose C_t is 2 orders of magnitude below that of NCSX. The reason why is shown in Fig. 2, which compares radial curvature $\kappa_1(\theta)$ for 1 poloidal transit for QA_35q (solid) with that for NCSX (dashed). One sees that Stellopt has found a means of boosting κ_1 so that it has bad curvature ($\kappa_1 < 0$) almost nowhere, and worse curvature than NCSX only where $\kappa_1 > 0$ for both configurations. While QA_35q has a κ_1 which is more oscillatory than for NCSX, it has a smooth, converged VMEC equilibrium, with boundaries of both shown in Fig. 3 for cross sections at 4 values of toroidal azimuth ζ.

While C_t has fallen by 2 orders of magnitude, the decisive test of whether QA_35q has transport truly diminished from NCSX is from nonlinear GENE runs. This comparison is given in Fig. 4, showing the line-averaged Q_{gk} for QA_35q (solid) and NCSX (dashed) versus time. One sees that QA_35q indeed has Q_{gk} substantially diminished from that for NCSX, by a factor of about 2.5, not nearly as large as that indicated by Q_{prox}, but still quite appreciable, comparable to the reduction achieved in tokamaks in going from L- to H-mode. Thus, while not highly accurate, this Q_{prox} is adequate to guide Stellopt in the direction desired.

QA_35q is a first "proof-of-principle" that substantial turbulence mitigation can indeed be achieved by this approach. However, in evolving QA_35q, Stellopt did not apply various constraints to the configurations to make them fully satisfactory. For example, while mostly ballooning stable, as is LI383, QA_35q is kink unstable, and its rotational transform has dropped from that of LI383 by a factor of about 2.7.

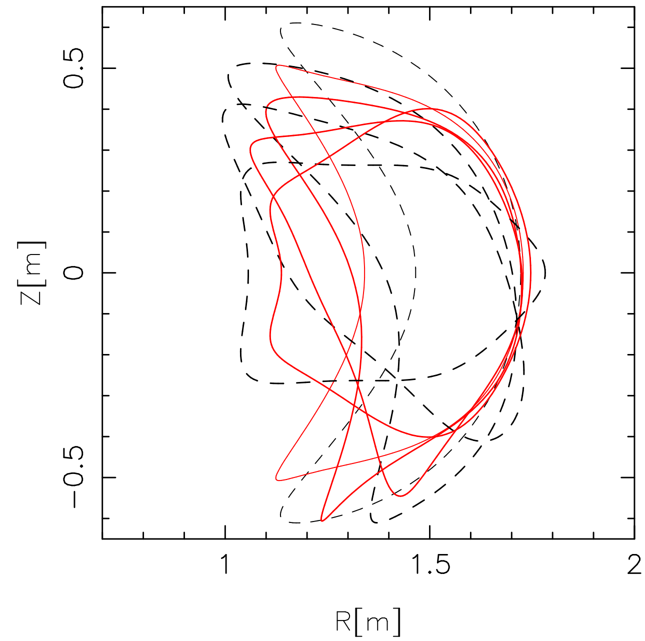

FIG. 3: (Color online) Comparison of boundary shapes of QA_35q (red solid) and NCSX (black dashed) at values of $N\zeta$ (= number of field periods × toroidal angle) $= 0, \pm\pi/2, \pi$.

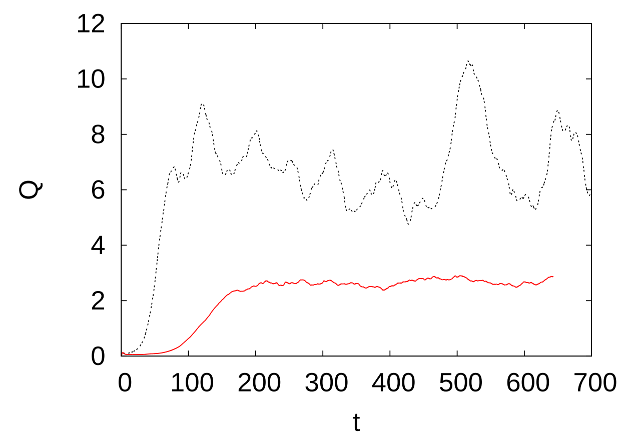

FIG. 4: (Color online) Comparison of line-averaged heat flux Q_{gk} versus time for QA_35q (red solid) and NCSX (black dashed) from nonlinear GENE runs. QA_35q achieves a reduction in turbulent transport over that in NCSX by a factor of about 2.5.

Many further possibilities exist for making use of this general approach to turbulent transport mitigation. The reduction Stellopt achieved in QA_35q principally made use of the κ_1-dependence of Q_{prox}, finding a means of deforming NCSX to restrict the domain of bad curvature, and thereby alleviate the ITG instability. In a similar way, one may seek other configurations which reduce transport by using the s_l-dependence in Q_{prox}. Also, as noted, the present Q_{prox} can be improved as a model for ITG transport, and one may expect further improvements would accrue as more of the significant physics in

Q_{gk} is captured by Q_{prox}. Further, the present restriction to ITG turbulence was taken only for simplicity – any modes which gk codes such as GENE can compute (*e.g.*, trapped-electron or electron temperature-gradient modes) can be addressed by this method, developing a modified Q_{prox} guided by theory and by gk studies of Q_{gk}. Moreover, it will also be of interest to use starting designs other than NCSX, to see what different means of achieving tranport reduction Stellopt finds as the initial configuration is varied. For example, each of the nc-transport-optimized designs studied in Ref. 9, and perhaps tokamaks, would provide an edifying testbed for this approach. Work addressing these avenues has been initiated.

Acknowledgment

The authors are grateful to A. Boozer, L. Maingi, G. Rewoldt, and E. Valeo for valuable discussions. This work supported by U.S.Department of Energy Contract No.DE-AC02-09CH11466.

[1] H.E. Mynick, T.K.Chu, A.H.Boozer, *Phys. Rev. Letters* **48**, 322 (1982).
[2] A.H. Boozer, Phys.Fluids **26** 496 (1983).
[3] J. Nührenberg, R. Zille, *Phys. Lett. A* **129**, 113 (1988).
[4] J. Nührenberg, W. Lotz, and S. Gori, in *Theory of Fusion Plasmas*, E. Sindoni, F. Tryon and J. Vaclavik eds., SIF, Bologna, (1994).
[5] P.R. Garabedian, *Phys. Plasmas* **3**, 2483 (1996).
[6] A. Reiman, G. Fu, S. Hirshman, L. Ku, *et al.*, *Plasma Phys. Control. Fusion* **41** B273 (1999).
[7] F. Jenko, W. Dorland, M. Kotschenreuther, B.N. Rogers, *Phys. Plasmas* **7**, 1904 (2000).
[8] P. Xanthopoulos, W. A. Cooper, F. Jenko, Yu. Turkin, A. Runov J. Geiger, *Phys. Plasmas* **16**, 082303 (2009).
[9] H.E. Mynick, P. Xanthopoulos and A.H. Boozer, *Phys.Plasmas* **16** 110702 (2009).
[10] F. Romanelli, *Physics of Fluids B* **1**, 1018 (1989).
[11] J. Garci'a, K. Yamazaki, J. Dies, J. Izquierdo, *Plasma physics and controlled fusion* **48**, p15-27, (2006).
[12] Wm. H. Press, *et al.*, *Numerical Recipes in Fortran 77*, (Cambridge University Press, 1996), p.436ff.
[13] G. Grieger, W. Lotz, P. Merkel, et al., *Phys. Fluids -B* **4**, 2081 (1992).
[14] Wm. H. Press, *et al.*, *Numerical Recipes in Fortran 77*, p.676ff.
[15] G.H. Neilson, M.C. Zarnstorff, J.F. Lyon, the NCSX Team, *Journal of Plasma and Fusion Research* **78**, 214-219 (2002).

The Princeton Plasma Physics Laboratory is operated
by Princeton University under contract
with the U.S. Department of Energy.

Information Services
Princeton Plasma Physics Laboratory
P.O. Box 451
Princeton, NJ 08543

Phone: 609-243-2750
Fax: 609-243-2751
e-mail: pppl_info@pppl.gov
Internet Address: http://www.pppl.gov